Efficiency Improvement at Light Load in Bidirectional DC-DC Converter by Utilizing Discontinuous Current Mode

Hoai Nam Le, Daisuke Sato, Koji Orikawa, Jun-ichi Itoh
Nagaoka University of Technology
1603-1 Kamitomioka-cho
Nagaoka city Niigata, Japan
Tel.: +81 / (258) – 47.9533.
Fax: +81 / (258) – 47.9533.
E-Mail: lehoainam@stn.nagaokaut.ac.jp
URL: http://itohserver01.nagaokaut.ac.jp/itohlab/index.html

Keywords

«Discontinuous Current Mode», «Bidirectional DC-DC Converter», «Nonlinearity Compensation»

Abstract

This paper proposes a feedback current control for bidirectional DC-DC converter which is operated in Discontinuous Current Mode (DCM) at light load and Continuous Current Mode (CCM) at heavy load in order to improve light load efficiency. In the proposed method, the nonlinearity compensation for DCM operation is constructed by using the duty ratio at previous calculation period. Moreover, the introduction of DCM current feedback control into bidirectional power conversion is accomplished by detecting the operation mode at the output of the control system. This make the control becomes parameter-independent. The validity of the proposed control is confirmed by a 1-kW prototype. In the ramp response, the slope of the DCM current almost agrees to the design value with the error of 0.8%. Moreover, the smooth transition among 4 current modes: CCM-powering, DCM-powering, DCM-generation, CCM-generation, is also confirmed. On the other hand, in order to further improve the efficiency at light load, the synchronous switching for DCM is proposed. As a result, at load of 0.1 p.u. the efficiency of the DCM synchronous switching is improved by 1.5% from 97.2% to 98.7% compared with the CCM synchronous switching. Besides, it is confirmed that, the efficiency of the CCM/DCM synchronous switching is higher by 0.2% than that of the CCM/DCM asynchronous switching at all range of load. Furthermore, the efficiency at rated load is 98.8%, whereas the maximum efficiency is 99.0% at load of 0.45-0.65 p.u..

I. Introduction

Recently, high power bidirectional DC-DC converters are widely applied to electric vehicles, and hybrid electric vehicles. This DC-DC converter is required to have small size and high efficiency. Generally, the Continuous Current Mode (CCM) control is applied in such converter due to its simple control. Nevertheless, because the current ripple in CCM is constant at all load range, it is difficult to achieve high efficiency at light load when the average current is low. Therefore, reducing the current ripple is the direct method to avoid the decrease of efficiency at light load. In order to reduce the current ripple, the conventional methods are increasing the inductance or the switching frequency [1]-[5]. However, when the circuit parameters have already been optimized at full load operation, any increase in inductance or switching frequency only leads to the increase in size of inductor or heat sink.

On the other hand, in the Discontinuous Current Mode (DCM) control, because the current ripple becomes smaller at light load, high efficiency can be maintained. Therefore, many papers in which CCM is applied at heavy load and DCM is applied at light load have been proposed [5]-[9]. In particular, it is well known that different operation modes can result in very different dynamics in the frequency domain [10]. The reason is that, in DCM the zero-current intervals which is dependent on the average current, introduces the nonlinearity to the duty-ratio-to-current transfer function. As the result, the conventional method to control CCM and DCM is using two controllers; one of which is designed based on the linear transfer function of CCM, whereas the other controller is designed based on the nonlinear transfer function of DCM [5]-[6]. However, when the current alternates between CCM and DCM, the current control performance worsens due to the initialization of the controller [11]. Therefore, the control of CCM and DCM without alternating controller is desired.

In this paper, the control method which uses only one PI controller for both CCM and DCM in order to achieve the high current control performance without alternating controller, is proposed. In order to control both CCM and DCM, a compensation part is introduced at the output of PI controller to compensate the nonlinearity in DCM. The compensation part is designed as a function of the duty ratio at previous sampling period, which makes the calculation for the compensation part become parameter-independent compared to [5]-[9]. This paper is organized as follows; first, the circuit model in CCM and DCM is derived. Second, the nonlinear part in DCM is linearized at stable points in order to design the compensation factors. Third, the technique to apply the proposed CCM/DCM controller in bidirectional current control is explained. Next, in order to further improve efficiency, the synchronous switching is applied to DCM by estimating the zero crossing point of the current. After that, the current response of the proposed control is verified by a 1-kW prototype. Finally, the comparison of efficiency among the DCM synchronous switching, the DCM asynchronous switching and the CCM synchronous switching is conducted to verify the efficiency improvement by applying the DCM synchronous switching.

II. Proposed CCM/DCM control method

A. Conventional CCM inner current loop design

Fig. 1 shows typical bidirectional DC-DC converter configuration. The average modeling technique is used to model the bidirectional DC-DC converter for the inner current control loop design [6]-[9]. The output voltage is assumed to be constant, because the response of the inductor current is much higher than that of the output voltage in outer voltage loop design step.

Fig. 2 shows the conventional inner current loop in CCM. In this paper, the closed loop of the inner

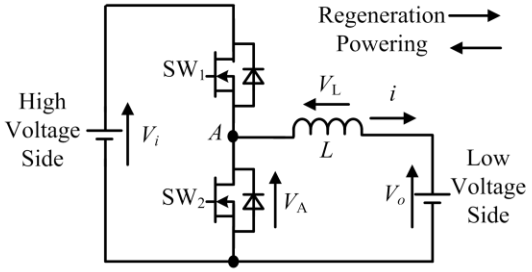

Fig. 1. Typical bidirectional DC-DC converter. Due to simple configuration, the above converter is widely applied in bidirectional power conversion.

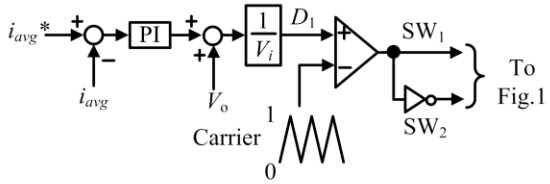

Fig. 2. Conventional inner current loop in CCM. Due to simple design and good performance, PI controller is widely used by power electronics engineers.

current loop is designed based on the second-order standard form. Hence, the coefficients of PI controller is designed as follows,

$$K_p = 2\xi\omega_n L \quad \text{.....(1)}$$

$$T_i = \frac{2\xi}{\omega_n} \quad \text{.....(2)}$$

where L is the inductance, K_p is the proportional gain, T_i is the integral period of PI controller, ω_n is the natural angular frequency, ζ is the damping factor, and ω_n, ζ are designed in order to achieve the desired inductor current response.

B. Proposed CCM/DCM inner current loop design

Fig. 3 shows inductor current waveform in DCM, where D_1, D_2 and D_3 denote the duty ratio of the first, the second and the zero-current interval respectively. A circuit model for both CCM and DCM is obtained as follows. First, the average current i_{avg} and the current peak i_{peak} can be expressed as,

$$i_{avg} = \frac{i_{peak}}{2}(D_1 + D_2) = \frac{i_{peak}}{2}(1 - D_3) \quad \text{.....(3)}$$

$$i_{peak} = \frac{V_i - V_o}{L} D_1 T_{sw} \quad \text{.....(4)}$$

where V_o, V_i are the output and input voltages, and T_{sw} is the switching period. Besides, the voltage V_A across the SW_2 and the voltage V_L across the inductor can be expressed as,

$$V_A = D_1 V_i + D_3 V_o \quad \text{.....(5)}$$

$$V_L = V_A - V_o \quad \text{.....(6)}$$

Substituting (3),(4), and (5) into (6),

$$V_L = D_1 V_i + [1 - \frac{2L}{(V_i - V_o)T_{sw}} \frac{i_{avg}}{D_1}] V_o - V_o \quad \text{.....(7)}$$

Then, the circuit model is established based on (7).

Fig. 4 shows circuit model of bidirectional DC-DC converter. In CCM, the dash line part does not exist, because the average current i_{avg} equals to the half current peak $i_{peak}/2$. On the other hand, in DCM, the voltage which occurs during the zero-current interval introduces the nonlinearity into DCM transfer function. This worsens the current response in DCM when same PI controller is applied for both CCM and DCM. Therefore, the output of PI controller is necessary to be compensated when the circuit is operated in DCM. The design of the compensation part for the nonlinearity of DCM is explained as follows. First, the circuit model in Fig. 4 is linearized at stable points.

Fig. 5 shows the linearized circuit model. In order to simplify the coefficients in the linearized circuit model, the relationship between such coefficients at stable points are derived as follows [7],

$$I_{avg\_s} = \frac{T_{sw}}{L} \frac{D_{1\_s}^{\ 2}}{2} \frac{V_i(V_i - V_o)}{V_o} \quad \text{.....(8)}$$

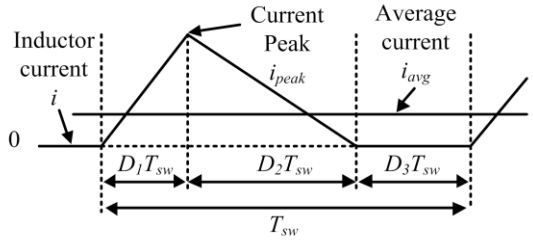

Fig. 3. Inductor current waveform in DCM. The zero-current interval makes it difficult to sample average current and introduces the nonlinearity into the duty-to-current transfer function.

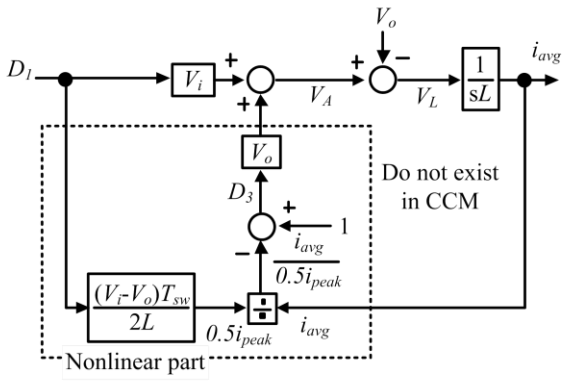

Fig. 4. Circuit model of boost converter in the DCM operation. The zero-current interval makes the duty-to-current transfer function become nonlinear.

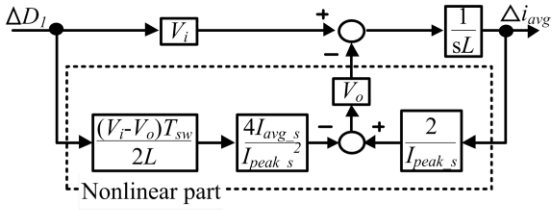

Fig. 5. Linearized circuit model. Controlling DCM by PI controller of CCM is achieved by compensating the nonlinear part at the output of PI controller.

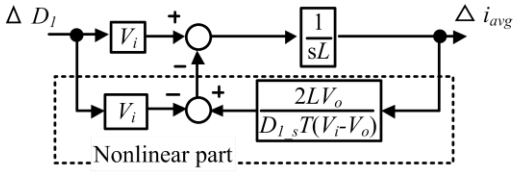

Fig. 6. Simplified and linearized circuit model. The duty ratio at steady-state operating points in the circuit model is approximated as the duty ratio at previous sampling period in order to eliminate the nonlinearity in DCM.

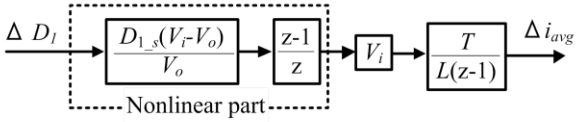

Fig. 7. Discretized circuit model. Utilizing the duty ratio at previous sampling period in order to eliminate the nonlinearity in DCM makes the controller parameter-independent.

$$I_{peak\_s} = \frac{V_i - V_o}{L} D_{1\_s} T_{sw} \quad \text{.....(9)}$$

where I_{avg_s}, I_{peak_s} and D_{1_s} are the average current, the peak current and the duty ratio of SW_1 at stable points, respectively. Then, (8) and (9) are substituted into Fig. 5 to express all coefficients as functions of D_{1_s}.

Fig. 6 shows the simplified circuit model. In order to eliminate the dash line part in Fig. 6, in the control system, the value of D_{1_s} is approximated as the duty ratio of SW_1 at previous sampling period $D_1[n\text{-}1]$. As the result, the circuit model is necessary to be analyzed in discrete model.

Fig. 7 shows the discretized circuit model. In order to use same PI controller of CCM for DCM, the dash line part in Fig. 7 is necessary to be set as unity when the circuit is operated in DCM. Therefore, in the control system, the inverse part of the dash line part in Fig. 7 is multiplied at the output of PI controller in order to compensate for the nonlinearity of DCM.

Fig. 8 shows the proposed CCM/DCM control. The compensated part to eliminate the nonlinearity in DCM, is arranged into two compensation factors K_{DCM} and a_{DCM} in order to simplify the control system. By introducing two compensation factors K_{DCM} and a_{DCM}, the integral part of the PI controller is not required to be initialized when current mode alternates between CCM and DCM. This ensures a smooth transition between DCM and CCM.

Table I shows the values of two compensation factors in case of CCM and DCM. When the circuit operates in CCM, all the compensation factors are set as unity. On the other hand, when the circuit operates in DCM, two compensation factors are calculated as in Table I.

C. Control of DCM current in bidirectional power conversion

Fig. 9 shows the circuit operating in either regeneration mode or powering mode when DCM asynchronous switching is applied. It can be understood that with same value of D_1, the operation mode is determined by driving one of switches and turning off the other switch. Therefore, it is necessary to determine which switching pattern should be used. This is accomplished as follows; different from CCM, in DCM the duty ratio D_1 is a function of average current i_{avg} as shown in (8). Hence, when the current becomes negative, the duty ratio D_1 also becomes negative. This problem can be overcome by output the absolute value of duty ratio to the switches. Furthermore, which switch is turned off in DCM asynchronous switching is determined by the state of duty ratio D_1.

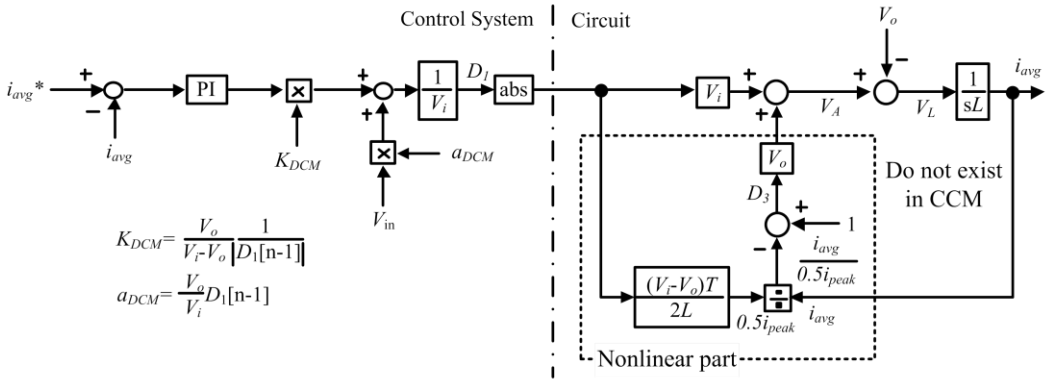

Fig. 8. Proposed CCM/DCM control system and circuit model. Smooth transition between CCM and DCM is achieved by compensating only the output of PI controller.

Table I. Values of two compensation factors.

Current Mode	CCM	DCM
a_{DCM}	1	$\frac{V_i D_1[n-1]}{V_o}$
K_{DCM}	1	$\frac{V_o}{(V_i-V_o)\lvert D_1[n-1]\rvert}$

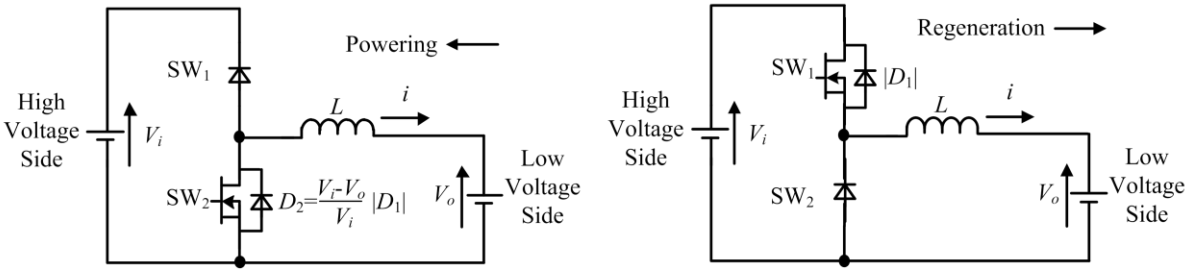

(a) DCM in powering mode (b) DCM in regeneration mode

Fig. 9. Operation of bidirectional DC-DC converter when DCM asynchronous switching is applied. Which mode the circuit is operated is determined by the output of the control system D_1 in Fig. 8.

Table II shows the duty ratios which are used to drive the switches in DCM regeneration mode and DCM powering mode. When the duty ratio D_1 from the control system in Fig.8 is negative, the circuit is operated in powering mode, which means SW_1 is turned off while SW_2 is driven by the duty ratio D_2 calculated as in Table II. On the other hand, when the duty ratio D_1 becomes positive, the circuit is operated in regeneration mode, which means SW_2 is turned off while SW_1 is driven by the duty ratio $|D_1|$. By using this method, the integral part of the PI controller is not required to be initialized when the current mode alternates between regeneration mode and powering mode.

D. Application of DCM synchronous switching

Because the mechanism of the DCM synchronous switching is same in both powering mode and regeneration mode, only the powering mode is explained.

Fig. 10 shows two switching patterns which occur in DCM when the switch (MOSFET) is operated instead of being turned off to use as the diode. This operation can improve the efficiency because the conduction loss of MOSFET is smaller than that of diode. In conclusion, this converter can realize three operation modes in light load depending on the turn on and off of SW_1; i) Simple CCM synchronous switching in which SW_1 is switched alternately to SW_2, ii) DCM asynchronous switching in which SW_1 is turned off in light load and iii) DCM synchronous switching in which SW_1 is turned on only during the second interval as shown in Fig. 3.

The boost inductor current of the simple CCM synchronous switching becomes continuous. Therefore, the boost inductor current ripple is constant. However, this results in high current ripple at light load, which makes the efficiency decrease. In order to improve the efficiency in light load, the DCM asynchronous switching is applied. Although the DCM asynchronous switching can reduce the boost inductor current in light load, the conduction loss of the body diode in the MOSFET is still high. In the DCM synchronous switching, if SW_1 is turned on exactly only during the second interval as shown in Fig. 3, the current flows through MOSFET. As a result, the conduction loss will be reduced. In order to apply the DCM synchronous switching, the duty ratio D_1 is calculated in the proposed DCM feedback control and (10) in the conventional DCM feedforward control [5], respectively.

$$D_{1\_conv.\_ff} = \sqrt{\frac{2Li^{*}_{avg}(V_{out} - V_{in})}{T^{2}_{sw\,in}}} \quad \text{.....(10)}$$

Table II. Duties to control switches for DCM regeneration mode and DCM powering mode in DCM asynchronous switching.

Asynchronous Switching	Regeneration ($D_1 < 0$)	Powering ($D_1 \geqq 0$)
Duty-to-SW1	$\lvert D_1 \rvert$	0
Duty-to-SW2	0	$\frac{\lvert D_1 \rvert (V_i - V_o)}{V_i}$

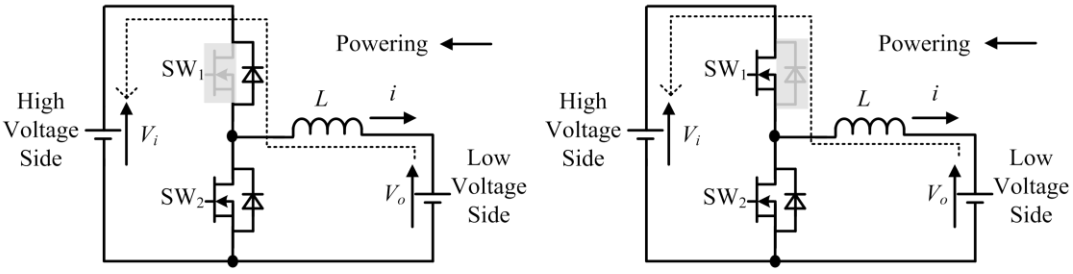

(a) DCM asynchronous switching (b) DCM synchronous switching

Fig. 10. DCM asynchronous switching and DCM synchronous switching in powering mode. Generally power loss emits when the current flows through MOSFET than diode. Therefore, the improvement in efficiency is expected when the synchronous switching is applied in DCM.

Table III shows the DCM synchronous switching in powering mode and regeneration mode. Because of the mismatch between the nominal values and the actual values, the duty ratio calculated from the feed forward control method in (10) makes SW_1 turn off too early or too late when the inductor current reaches zero. This leads to the increase of switching losses and conduction losses. On the other hand, the duty ratio D_1 calculated from the feedback control method represents precisely for the value of the inductor current. This enables SW_1 to be turned off exactly at the moment the inductor current reaches zero, which results in Zero Current Switching (ZCS). Because generally lower loss emits when the current flows through MOSFET than diode, the improvement of the efficiency is expected when the DCM synchronous switching is applied. Besides, it is noted in Table III that, in powering mode and regeneration mode, the turn on order of the switches for the DCM synchronous switching is different.

III. Experimental Results

Table IV shows the parameters in experiments. In this chapter, first, the experiment of the current ramp response is conducted in order to confirm the operation of the proposed CCM/DCM current feedback control in bidirectional power conversion. Next, the waveform of the current and the switching signal when the circuit is operated at the DCM synchronous switching is shown. Finally, the comparison of the efficiencies at light load among the CCM synchronous switching, the DCM synchronous switching, and the DCM asynchronous switching is conducted.

A. Current ramp response

The current ramp response of the current control block in Fig. 8 is confirmed. The incline of the ramp command is the maximum controllable values $(\mathrm{d}i_{avg}^*/\mathrm{d}t)_{\max}$ of the designed PI controller and is calculated as,

Table III. Duties to control switches for DCM regeneration mode and DCM powering mode in DCM synchronous switching.

Synchronous Switching	Regeneration ($D_1<0$)	Powering ($D_1 \geqq 0$)
Duty-to-SW1	$\lvert D_1 \rvert$ (*)	$\lvert D_1 \rvert$
Duty-to-SW2	$\frac{\lvert D_1 \rvert (V_i - V_o)}{V_i}$	$\frac{\lvert D_1 \rvert (V_i - V_o)}{V_i}$ (*)

(*): This switch needs to be turned on first in each mode.

Table IV. Parameters in experiments.

V_i	Input Voltage	350 V
V_o	Output Voltage	200 V
P	Rated Output Power	1 kW
f_{sw}	Switching Frequency	20 kHz
$f_{sampling}$	Sampling Frequency	20 kHz
L	Inductance	1080 μH
f_c	Cutoff frequency of PI controller	500 Hz
ζ	Damping factor of PI controller	0.707
Current command in Light Load		-1.6 A→1.6 A
Maximum controllable slope		3.55 A/ms
Current command in Full Load		-5.0 A→ 5.0 A
Current density		4 A/mm^2
Gap length		0.7 mm
Winging turn		46
Inductor core		PC40EI90
Switching device		TPH3006PS

$$\left(\frac{di_{avg}^*}{dt}\right)_{\max} = \frac{\omega_n \Delta i_{avg}^*}{2\sqrt{2}} \quad \text{.....(11)}$$

where Δi_{avg}^* is the amplitude of current command.

Fig. 11 shows the ramp response of inductor current by the conventional CCM control and the proposed CCM/DCM control. At light load, the variation width of current command is 3.2 A. Hence, the maximum controllable ramp command is 3.55 A/ms. It is concluded from Fig. 11(a), (b) that the DCM response is almost as same as the designed value with error of 0.8%, whereas the error of the CCM response is 7.6%. It is understood that the ripple of the current in DCM is reduced compared to CCM, which leads to the reduction of loss at light load. This also results in the better control performance in DCM operation. On the other hand, the detection of CCM and DCM in this paper is to compare the feedback current with the value of the current at the boundary between CCM and DCM. It is confirmed from Fig. 11(c) that the current smoothly alternates among 4 current modes; CCM regeneration, DCM regeneration, DCM powering and CCM generation. By those results, the validity of the proposed CCM/DCM control for bidirectional power conversion is confirmed.

B. DCM synchronous switching operation and efficiency comparison

Fig. 13 shows the synchronous switching waveforms in DCM powering. It is concluded that SW_1 is turned off exactly when the current reaches zero, which achieves ZCS. Furthermore, before SW_1 is turned on, during the dead time, the current flows through the diode. Therefore, SW_1 turns on at the forward voltage of the diode. Therefore, ZVS is achieved when SW_1 is turn on. In summary, the synchronous switching in DCM causes almost no switching loss in SW_1.

Fig. 14 shows the efficiency comparison among the CCM synchronous switching, the DCM synchronous switching, and the DCM asynchronous switching. The efficiency of the CCM/DCM synchronous switching and the CCM synchronous switching at full load are same as 98.8% because the

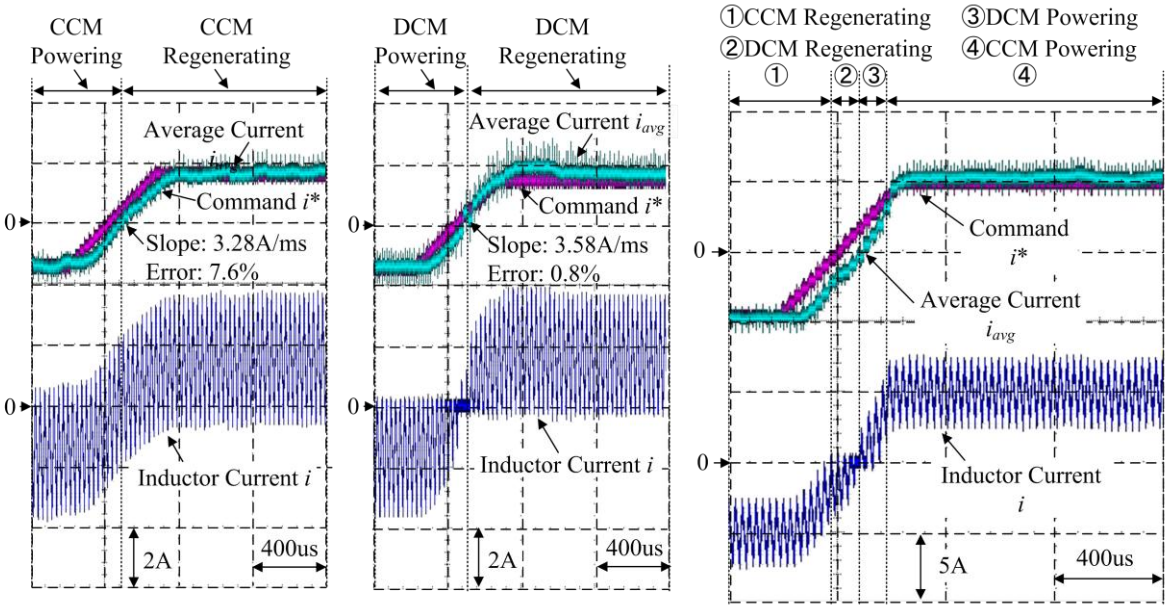

(a) CCM operation at light load (b) DCM operation at light load (c) CCM/DCM operation at full load

Fig. 11. Current ramp response of conventional CCM control and proposed CCM/DCM control at light load and full load. The current response of DCM control is almost as same as the design value with error of 0.8%. Because the current ripple of DCM is reduced at light load, the high efficiency can be maintained at all load range. Besides, the smooth transition among 4 current modes: CCM regeneration, DCM regeneration, DCM powering and CCM powering is confirmed.

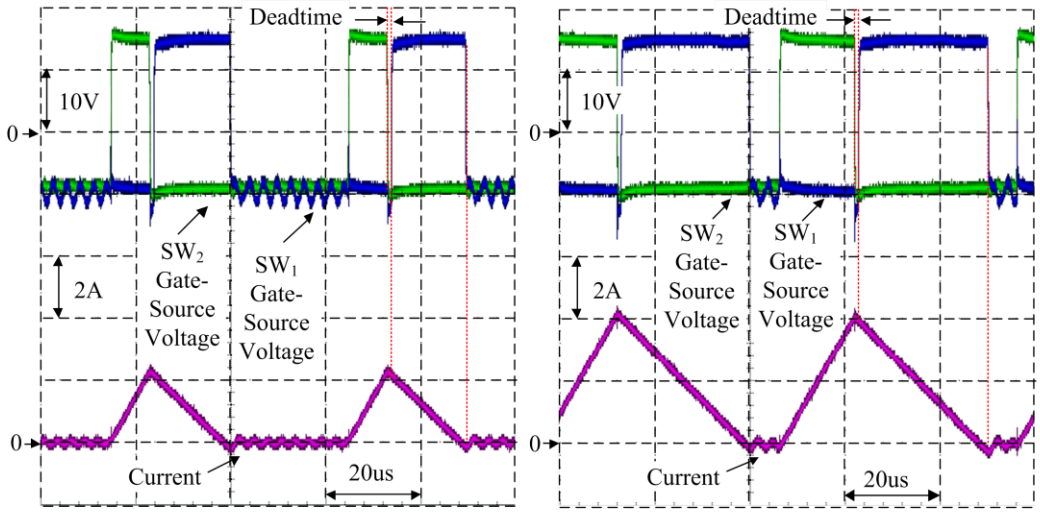

(a) At load of 0.2 p.u. (b) At load of 0.4 p.u.

Fig. 13. DCM synchronous switching in powering mode. SW_1 is turned off exactly when the current reaches zero. This achieves ZCS. Furthermore, before SW_1 is turned on, during the deadtime, the current flows through diode. Therefore, SW_1 turns on at the forward voltage of diode. This achieves ZVS. To sum up, the DCM synchronous switching causes almost no switching loss in SW_1.

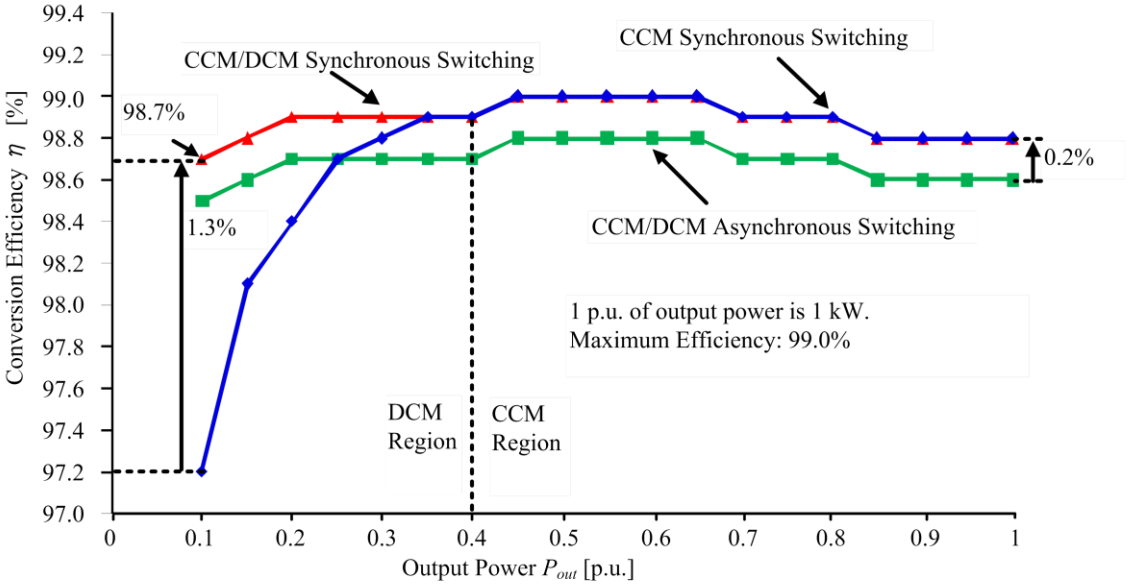

Fig. 14. Efficiencies among CCM synchronous switching, CCM/DCM synchronous switching and CCM/DCM asynchronous switching. Due to the reduced current ripple at light load, the efficiency in the CCM/DCM synchronous switching is improved by 1.3% compared to the CCM synchronous switching. Besides, by applying the synchronous switching into DCM, the efficiency is improved by 0.2% compared to the asynchronous switching.

circuit is designed in order to operate in CCM at full load. When the load becomes lighter, whereas the efficiency of the CCM synchronous switching decreases as explained in Fig. 11, the efficiency of the DCM synchronous switching is still maintained at high values over than 98.7%. Specifically, at load of 0.1 p.u., the efficiency is improved by 1.3% when the DCM synchronous switching is applied. This efficiency improvement especially benefits the application with a frequent variation between light load operation and full load operation. On the other hand, compared to the CCM/DCM asynchronous switching, the efficiency of the CCM/DCM synchronous switching is higher by 0.2% at all load range.

This efficiency improvement is because the conduction loss of MOSFET is lower than that of a diode in this case. However, the conduction loss in the DCM synchronous switching increases with the square of the current, whereas the conduction loss in the DCM asynchronous switching increases with the current. Therefore, there might be case that the efficiency of the DCM synchronous switching is lower than one of the DCM asynchronous switching. It can be concluded that the DCM synchronous switching benefits mostly the switching device with a small on-resistance in the MOSFET part and a high forward voltage in the parasitic diode such as SiC-MOSFET. Furthermore, the maximum efficiency reaches 99.0% at load of 0.45-0.65 p.u.. From these results, the effectiveness of the DCM application into bidirectional power conversion is confirmed.

IV. Conclusion

This paper proposed the CCM/DCM control method for bidirectional DC-DC converter. The nonlinearity of DCM was compensated by the utilization of the duty ratio at the previous calculation period. On the other hand, the detection of powering mode and regeneration mode in order to apply DCM was accomplished by observing the state of the duty ratio. In the experimental current ramp response, the error of the DCM current response was 0.8%, and the smooth transition of the current among 4 current modes: CCM regeneration, DCM regeneration, DCM powering and CCM powering was also confirmed. Moreover, in order to further improve the efficiency at light load, the synchronous switching was applied into DCM. As the results, the efficiency of above 98.7% was maintained at all load range from 0.1 p.u. to 1.0 p.u..

In future work, the technique to control both CCM and DCM independently from the value of inductance will be explained. Furthermore, the design of the current ripple and the switching frequency will be conducted. The power density of the bidirectional DC-DC converter will be optimized based on pareto-front curve.

References

[1] R. C. N. Pilawa-Podgurski, A. D. Sagneri, J. M. Rivas, D. I. Anderson, D. J. Perreault, “Very-High-Frequency Resonant Boost Converters”, Transactions on Power Electronics, Vol. 24, No. 6, pp. 1654-1665, 2009.

[2] Ch. Huang, P. K. T. Mok: “An 84.7% Efficiency 100-MHz Package Bondwire-Based Fully Integrated Buck Converter With Precise DCM Operation and Enhanced Light-Load Efficiency”, Journal of Solid-State Circuits, Vol. 48, No. 11, pp. 2895-2607, 2013.

[3] Y. P. Su, Y. K. Luo, Y. Ch. Chen, K. H. Chen: “Current-Mode Synthetic Control Technique for High-Efficiency DC–DC Boost Converters Over a Wide Load Range”, Transactions on VLSI Systems, Vol. 22, No. 8, pp. 1666-1678, 2013.

[4] J. Itoh, K. Matsuura, K. Orikawa, “Reduction of a Boost Inductance using a Switched Capacitor DC-DC Converter”, in 8th International Conference on Power Electronics and ECCE Asia, Jeju, May 30 -June 3, 2011, pp. 1315-1322.

[5] J. Zhang, J. Sh. Lai, R. Y. Kim, W. Yu, “High-Power Density Design of a Soft-Switching High-Power Bidirectional dc–dc Converter”, Transactions on Power Electronics, Vol. 22, No. 4, pp. 1145-1153, 2007.

[6] T. S Hwang, S. Y. Park, “Seamless Boost Converter Control Under the Critical Boundary Condition for a Fuel Cell Power Conditioning System”, Transactions on Power Electronics, Vol. 27, No. 8, pp. 3616-3626, 2012.

[7] K. D. Gusseme, D. M. V. de Sype, A. P. V. den Bossche, J. A. Melkebeek, “Digitally Controlled Boost Power-Factor-Correction Converters Operating in Both Continuous and Discontinuous Conduction Mode”, Transactions on Power Electronics, Vol. 52, No. 1, pp. 88-97, 2005.

[8] Sh. F. Lim, A. M. Khambadkone, “A Simple Digital DCM Control Scheme for Boost PFC Operating in Both CCM and DCM”, Transactions on Power Electronics, Vol. 47, No. 4, pp. 1802-1812, 2011.

[9] C. W. Clark, F. Musavi, W. Eberle, “Digital DCM Detection and Mixed Conduction Mode Control for Boost PFC Converters”, Transactions on Power Electronics, Vol. 29, No. 1, pp. 347-355, 2014.

[10] J. M. Blanes, R. Gutierrez, A. Garrigos, J. L. Lizan, J. M. Cuadrado, “Averaged Modeling of PWM Converters Operating in Discontinuous Conduction Mode”, Vol. 16, No. 4, pp. 482-492, 2001.

[11] R. W. Erickson and D. Maksimovic, Fundamentals of Power Electronics, 2nd ed. New York: Springer-Verlag, 2001.